Vibrational Spectroscopic Study on Trigonal Poly(oxymethylene) Consisting of the Extended Chain Morphology

Hirofumi Morishita,† Masamichi Kobayashi,* and Fumitoshi Kaneko

Department of Macromolecular Science, Faculty of Science, Osaka University, Toyonaka, Osaka 560, Japan

Received May 25, 1994®

ABSTRACT: The moth-shaped single crystals of trigonal poly(oxymethylene) consisting of extended chains (ECC) were obtained by the thermal phase transition of single crystals of orthorhombic poly(oxymethylene) having the same crystal habits. Polarized Raman spectra of the trigonal poly(oxymethylene) single crystals have been taken by means of the microprobe technique. Ordinary right-angle polarized Raman spectra have been measured on pressurized superdrawn filaments of trigonal poly(oxymethylene) having high transparency and ECC-type crystal morphology. Assignments of the Raman-active modes including the E_2 vibrations, which mostly remain unassigned so far, have been performed on the basis of the observed polarizations. The $E_1(7)$ and $E_1(8)$ modes exhibit the LO (longitudinal optic)–TO (transverse optic) splitting characteristic of the noncentrosymmetric crystal lattice. In order to confirm the splittings, the angular dispersion of the LO component has been measured.

Introduction

Trigonal poly(oxymethylene)[1-3] (abbreviated as t-POM) is obtained exclusively through the ordinary crystallization processes from the melt or dilute solutions.

Two decades ago, Iguchi et al. obtained feather-shaped[4,5] and needlelike single crystals[6,7] of t-POM consisting of fully extended chains (ECC). They were generated in a heterogeneous cationic polymerization system of trioxane in cyclohexane solution using boron trifluoride and water as catalyst. Typical folded-chain crystals (FCC) of t-POM having a hexagon plate shape with a lamella thickness of about 10 nm were grown from dilute bromobenzene solutions.[8-10]

Infrared and Raman spectra of normal and deuterated poly(oxymethylene) (t-POM-d_2) have been investigated by many workers from structural and analytical viewpoints.[11-16] For the normal mode analysis of molecular vibrations and the study of molecular orientation, polarized spectral data are of essential importance. Polarized infrared spectra of oriented films of t-POM and t-POM-d_2 have been measured, and vibrational assignments of the zone-center fundamentals have been fully established by the normal mode analysis based on the polarization data.[12] On the contrary, polarization measurement of Raman spectra of t-POM has been extremely difficult, because drawn fibers of commercially available t-POM samples and superdrawn fibers of t-POM produced by the microwave heating method[13] were opaque and therefore polarizations of the incident and scattered lights were strongly scrambled. Thus, all the Raman spectra of t-POM reported so far were unpolarized. Most of the infrared-inactive and Raman-active E_2 modes[14-16] of t-POM and t-POM-d_2 were not observed so far.

Recently, we found that on heating above 69 °C, single crystals of orthorhombic poly(oxymethylene) (o-POM) transformed to the t-POM phase, keeping the original crystal habit and the molecular orientation unaltered.[17,18] Thus, we obtained moth-shaped single crystals of t-POM having size and optical clearness suitable for the polarized micro-Raman measurement.[19]

Another method for obtaining well-oriented and highly crystalline transparent samples of t-POM has been developed by Komatsu et al.[20,21] They succeeded in producing superdrawn filaments containing few voids by stretching POM resin under high pressure. With such samples we are able to measure polarized Raman spectra by the oridinary right-angle scattering.[22]

Another unsolved problem of t-POM is concerned with the handedness of the helical molecules in the lattice. Crystallographically, the most reliable spece group of the t-POM lattice is $P3_1$-C_3^2 or $P3_2$-C_3^3 with the unit cell containing one molecule of a right-handed or left-handed helix. Therefore, the unit cell should be noncentrosymmetric (or chiral). However, there is still uncertainty in the chirality of the unit cell because of difficulty in determining the respective positions of the O and C atoms caused by the isoelectric nature of the O atom and CH_2 group. In fact, the precise value of the azimuthal angle with respect to the a axis has not been determined yet. The absence or presence of the inversion center in the space group is confirmable spectroscopically by observing the phenomenon of the LO (longitudinal optic)–TO (transverse optic) splitting of the Raman bands which belonging to the polar (infrared-active) phonons. For t-POM, the E_1 bands belong to this category.

Table 1. Factor Group Analysis of t-POM Crystal

phase angle (deg)	species	no. of normal modes	polarization[a] IR	Raman
0	A_1	5	forbidden	$(\alpha_{aa} + \alpha_{a^*a^*}), \alpha_{cc}$
0	A_2	5	μ_c	forbidden
$10\pi/9$	E_1	11×2	(μ_a, μ_{a^*})	$(\alpha_{ac}, \alpha_{a^*c})$
$20\pi/9$	E_2	12×2	forbidden	$(\alpha_{aa} - \alpha_{a^*a^*}, \alpha_{aa^*})$
$30\pi/9$	E_3	12×2	forbidden	forbidden
$40\pi/9$	E_4	12×2	forbidden	forbidden

[a] a^*: the perpendicular direction to the ac plane.

Experimental Section

A. Samples. Needlelike single crystals[23-27] (polymer whiskers) of t-POM and t-POM-d_2 were supplied from the Research Institute for Polymers and Textiles. These crystals were of hexagon shape with dimensions of about 2 μm in diameter and 100 μm in length.

Moth-shaped single crystals of t-POM[19,28] were obtained by the thermally induced solid-state phase transition of o-POM crystals having the same habits (refer to Figure 1 of ref 17). The resultant single crystals showed clearly optical birefrigence. As for the scattering geometry of the micro-Raman experiment, we

† Present address: Faculty of Education, Nagasaki University, Nagasaki-City, Nagasaki 852, Japan.

® Abstract published in *Advance ACS Abstracts,* August 15, 1994.

0024-9297/94/2227-5907$04.50/0

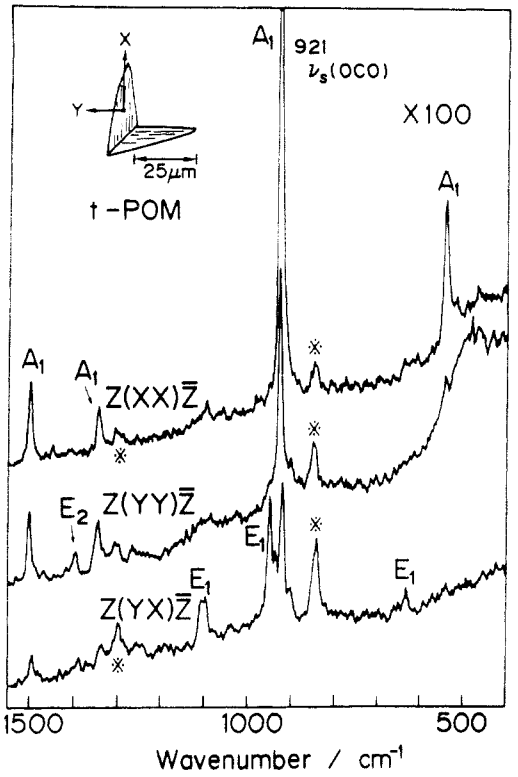

Figure 1. Polarized micro-Raman spectra of a moth-shaped single crystal of trigonal poly(oxymethylene). Bands marked with asterisks are spoiled bands by the objective itself.

defined the sample-fixed Cartesian coordinates for the moth-shaped single crystal as follows: X is parallel to the striations seen on the crystal face, Y is perpendicular to it within the plate surface, and Z is normal to the plate surface.

Pressurized superdrawn filaments (with the elongation ratio $\lambda = 19$) were produced by Asahi Chemical Co. Ltd. We used the rectangular filament with 2 mm width and 0.8 mm thickness for the polarization Raman measurements. The filament was cut into a 10 mm length, and the cut surface was polished with fine carborundum until the surface became clear. The sample-fixed Cartesian coordinates of this filament were defined as follows: X is parallel to the elongation direction (the c axis), Y is perpendicular to it within the wide surface, and Z is normal to the XY plane.

B. Vibrational Spectral Measurements. Ordinary right-angle Raman spectra of t-POM samples were taken with a JASCO R-500 monochromator using the 514.5 or 488.0 nm (Ar^+) excitation laser beam. For the Raman measurement at low temperature, an Oxford continuous flow-type cryostat was used.

Angular dispersion of the LO components of the $E_1(7)$ and $E_1(8)$ bands was measured on a superdrawn filament with the following geometry: The X axis of the sample was placed parallel to the scattering plane constructed with the incident $\mathbf{q}_i$ and scattered photon $\mathbf{q}_s$ propagation vectors ($\mathbf{q}_i \perp \mathbf{q}_s$), and the angle θ between the X axis and the phonon propagation vector $\mathbf{q} = \mathbf{q}_i - \mathbf{q}_s$ was set at 0, 45, and 90° by rotating the sample around the Y axis set perpendicular to the scattering plane. The Y-polarized incident beam was used, and the scattered light polarized parallel to $\mathbf{q}_i$ was collected (cf. Figure 5a).

Micro-Raman spectra of one t-POM single crystal were taken with an epi-illumination optical microscope (Olympus BH-2) attached to a JASCO NR-1000 double monochromator of 100 cm focal length using the 514.5 nm excitation source.

Results and Discussion

A. Polarized Vibrational Spectra of t-POM. The t-POM unit cell belongs to the space group $P3_1$-C_3^2 (or $P3_2$-C_3^3) and contains one 9/5 helical molecule having the $D(10\pi/9)$ line group symmetry which is ismorphous with the D_9 point group. The zone-central normal modes of the 9/5 helical molecule of t-POM are classified into six

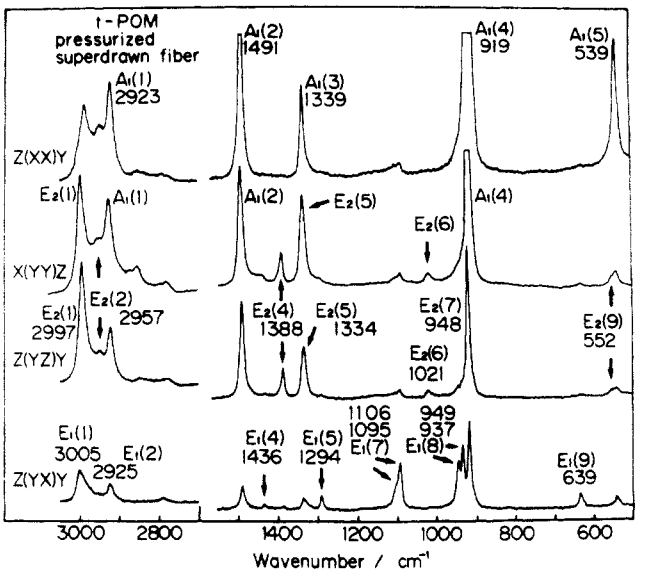

Figure 2. Polarized Raman spectra of a pressurized superdrawn filament of trigonal poly(oxymethylene).

Table 2. Raman and Infrared Vibrational Spectra of t-POM

	frequencies (cm^{-1})		
	obsd		
modes	Raman	IR	calcd
$A_1(1)$	2923, XX,[a] m[b]		2924[c]
$A_1(2)$	1491, XX, vs		1508
$A_1(3)$	1339, XX, s	inactive	1330
$A_1(4)$	919, XX, vs		916
$A_1(5)$	539, XX, s		587
$A_2(1)$		2985[d]	2977
$A_2(2)$		1358	1425
$A_2(3)$	inactive	1093	1118
$A_2(4)$		895	922
$A_2(5)$		220	237
$E_1(1)$	3005, YX, m	2999	2982
$E_1(2)$	2925, YX, m	2928	2926
$E_1(3)$	1468[e]	1470	1506
$E_1(4)$	1436, YX, w	1435	1407
$E_1(5)$	1294, YX, m	1292,[f] $\perp$[g]	1318
$E_1(6)$	1230, YX, vw	1240	1169
$E_1(7)$	1106, YX, vw		
	1095, YX, m	1093	1072
$E_1(8)$	949, YX, w		
	937, YX	938	930
$E_1(9)$	639, YX, m	633	634
$E_1(10)$	462, YX, vw	457	483
$E_1(11)$	40, YX, m		22
$E_2(1)$	2997, YZ, s		2978[h]
$E_2(2)$	2957, YZ, m		2897
$E_2(3)$	1482[e]		1498
$E_2(4)$	1388, YZ, m		1393
$E_2(5)$	1334, YZ, sh		1334
$E_2(6)$	1021, YZ, w	inactive	1133
$E_2(7)$	948, YZ, vw		938
$E_2(8)$	907[e]		912
$E_2(9)$	552, YZ, vw		555
$E_2(10)$	198, YZ, vw		189
$E_2(11)$			176
$E_2(12)$	65, YZ, m		56

[a] Polarizations. [b] Relative intensity: vs, very strong; s, strong; m, medium; w, weak; vw, very weak; sh, shoulder. [c] Refer to ref 12. [d] Refer to ref 24. [e] Needle crystal's data (at liquid He temperature). [f] Pressurized superdrawn filament's data. [g] Polarization: $\perp$, perpendicular. [h] Refer to ref 16.

symmetry species. The number of normal modes and the infrared and Raman polarizations for each symmetry species are summarized in Table 1. In the table, c and a denote the crystal axes of the trigonal lattice, and a^* is the axis perpendicular to the ac plane. In what follows, the

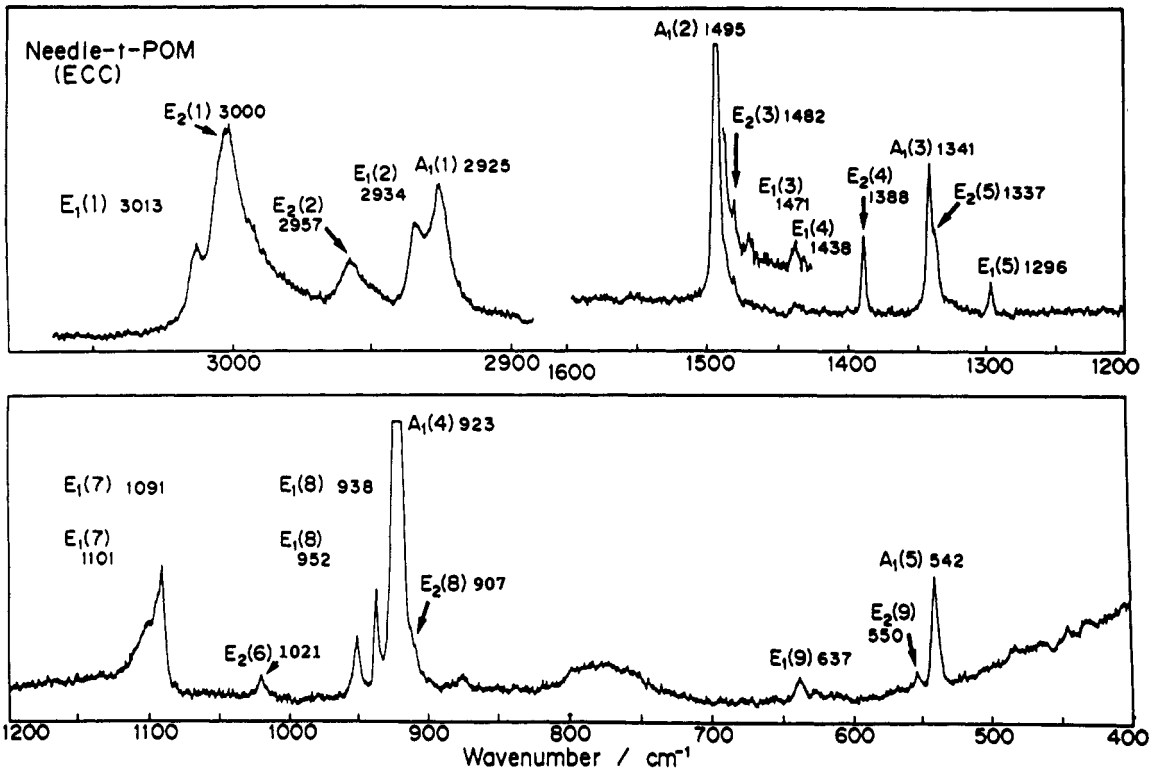

Figure 3. Raman spectra of needlelike single crystals of trigonal poly(oxymethylene) at liquid He temperature.

optically active fundamentals are designated as $A_1(m)$ (m = 1–5), $A_2(m)$ (m = 1–5), $E_1(m)$ (m = 1–11), and $E_2(m)$ (m = 1–12), the number m being the mode in the order of higher to lower frequency.

Figure 1 shows polarized micro-Raman spectra of a moth-shaped t-POM single crystal. All the sharp bands appearing in the (XX) spectrum are assigned to the A_1 species in reference to previous results of t-POM.[12] Especially, the strongest 921 cm^{-1} band is assigned to $A_1(4)$, the OCO symmetric stretch ν_s(OCO), which has a large α_{CC} Raman tensor element compared with the other vibrational modes. This shows that the X direction is parallel to the crystallographic c axis. This is confirmed by measuring the polarized spectra of one needlelike single crystal,[6,7] whose long axis has been determined to be parallel to the c axis. The bands appearing in the (YX) [i.e., the (ac) and (a^*c)] spectrum should be assigned to the E_1 modes; the bands at about 1100, 940, and 640 cm^{-1} are assigned to $E_1(7)$, $E_1(8)$, and $E_1(9)$. The E_2 modes including α_{aa}, α_{aa^*}, and $\alpha_{a^*a^*}$ elements are expected to appear in the (YY) spectrum, but not in (XX) and (YX). The 1387 cm^{-1} band observed in (YY) was assigned to $E_2(4)$, as suggested by previous workers.[15,16]

Figure 2 shows ordinary right-angle polarized Raman spectra of the pressurized superdrawn filament. All the sharp bands appearing in the (XX) spectrum should be assigned to the A_1 species. The bands observed in the (YX) spectrum appear at the same frequencies as the infrared perpendicular E_1 bands and are assigned undoubtedly to the E_1 species. The E_2 modes of an (n/m) uniform helix (with $n > 5$) are potentially Raman active. However, in most cases they are too weak to be detected. From the group theoretical consideration the E_2 modes are observed in the (YY) and/or (YZ) spectra, and not observed in (XX). The polarized Raman spectral data obtained for the superdrawn filament are summarized in Table 2.

B. E_2 Modes of t-POM and t-POM-d_2. In order to measure the weak E_2 bands more definitely, Raman spectra were taken on highly crystalline needlelike single crystals

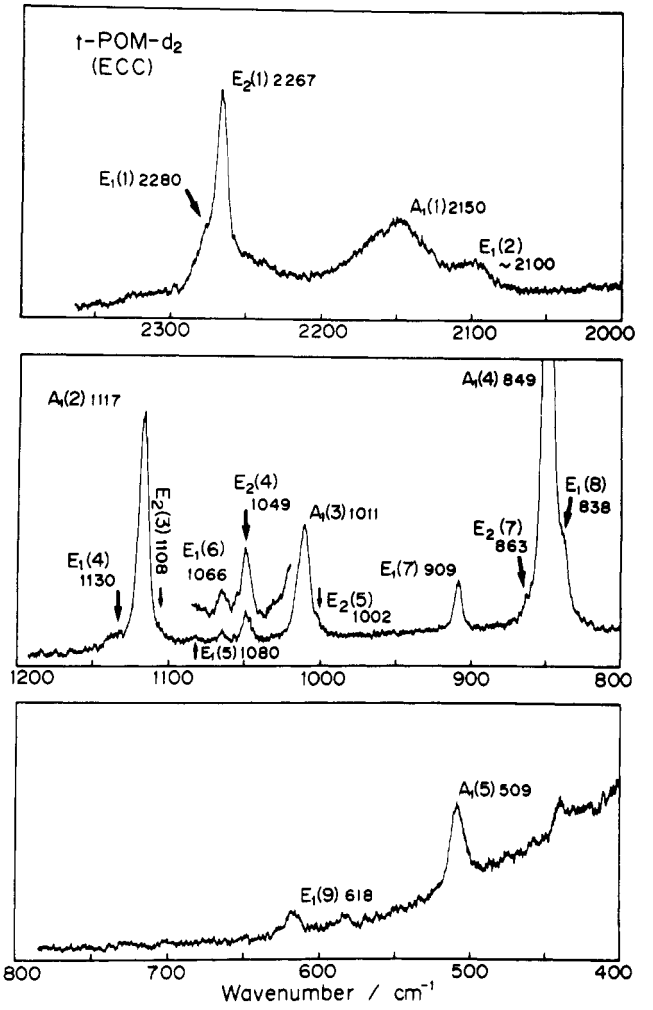

Figure 4. Raman spectra of needlelike single crystals of deuterated poly(oxymethylene).

of POM (at liquid He temperature) and POM-d_2 (at room temperature) samples, as shown in Figures 3 and 4. In

Table 3. Raman and Infrared Vibrational Spectra of t-POM-d_2

modes	frequencies (cm^{-1}) obsd Raman	obsd IR	calcd
$A_1(1)$	2150		2121[a]
$A_1(2)$	1117		1126
$A_1(3)$	1011	inactive	1013
$A_1(4)$	849		828
$A_1(5)$	509		557
$A_2(1)$			2193
$A_2(2)$		1048[b]	1154
$A_2(3)$	inactive	958	1026
$A_2(4)$		830	769
$A_2(5)$		199	212
$E_1(1)$	2280		2207
$E_1(2)$	~2100		2121
$E_1(3)$		1159[b]	1178
$E_1(4)$	1130	1127	1145
$E_1(5)$	1080	1083	1047
$E_1(6)$	1066	1065	1044
$E_1(7)$	909	908	916
$E_1(8)$	838	840	810
$E_1(9)$	618	617	618
$E_1(10)$		365	372
$E_1(11)$			21
$E_2(1)$	2267		2227[c]
$E_2(2)$			2122
$E_2(3)$	1108		1112
$E_2(4)$	1049		1057
$E_2(5)$	1002		1014
$E_2(6)$		inactive	994
$E_2(7)$	863		842
$E_2(8)$			830
$E_2(9)$			518
$E_2(10)$			183
$E_2(11)$			158
$E_2(12)$	58[d]		51

[a] Refer to ref 12. [b] Refer to ref 24. [c] Refer to ref 16. [d] Refer to ref 15.

Figure 3, the bands marked with arrows are assigned to the E_2 modes on referring to the Raman polarization data of the superdrawn filament. The assignments and frequencies of the bands are described in the figure.

As for the vibrational assignments of t-POM-d_2, infrared-active A_2 and E_1 modes have already been established, and distinct Raman bands have been assigned to the A_1 or E_1 modes,[12] except for the 1049 and 2267 cm^{-1} bands which are assigned to the $E_2(1)$ and $E_2(4)$ modes. Little has been known about the E_2 modes of t-POM-d_2 except for the 57 cm^{-1} band due to the $E_2(12)$ band.[15] There are observed three very weak E_2 Raman bands, as marked in Figure 4. The spectral data for POM-d_2 are summarized in Table 3.

C. LO–TO Splitting of the E_1 Bands of t-POM. In Figures 1 and 2, there are observed doublets around 1100 and 940 cm^{-1} in the (XY) spectrum. The low-frequency components of the doublets at 1095 and 937 cm^{-1} are assigned to the TO bands of the $E_1(7)$ and $E_1(8)$ modes, respectively, since the frequencies are the same as the corresponding infrared perpendicular bands. We consider that the high-frequency components at 1106 and 949 cm^{-1} should be assigned to the LO bands of the respective modes. Crystallographically, the t-POM lattice belongs to a noncentrosymmetric space group, containing one molecule passing through the unit cell. Therefore, in theory, one crystallite should be chiral, consisting of only left-handed or right-handed molecules. However, in actual samples the chirality is possibly diminished by structural defects involved and molecular motions. The appearance of the LO bands suggests that chirality of the lattice is held at least within each crystal domain. In order to confirm further the fact that the doubling of the E_1 Raman bands is caused by the LO–TO splitting, we tried to observe the angular dispersion of the LO bands. For the doubly degenerated E_1 modes, the position of the high-frequency component moves from the LO to the TO frequency, as the angle θ between the phonon propagation vector $\mathbf{q}$ and c axis varies from 90 to 0°, while the low-frequency component remains unshifted at the TO frequency (Figure 5a). At $\theta = 90°$ the high-frequency component appears at the highest frequency corresponding to the LO frequency, at $\theta = 45°$ it moves to a position between the LO and TO frequencies (the oblique phonon), and at $\theta = 0°$ only the low-frequency component appears. The experimental result is shown in Figure 5b. Although the expected frequency shift of the high-frequency component was not observed so clearly for the two E_1 modes, their intensities decreased as θ moved from 90 to 0°. This suggests that the main part of the high-frequency component moves as the theory predicts, but some part remains unshifted. The latter part may be due to the opaqueness of the sample that causes scrambling in the directions of the $\mathbf{q}_i$ as well as $\mathbf{q}_s$ vectors. Consequently, the observed spectral change is regarded to arise from the angular dispersion of the E_1 modes, supporting the noncentrosymmetric lattice of t-POM.

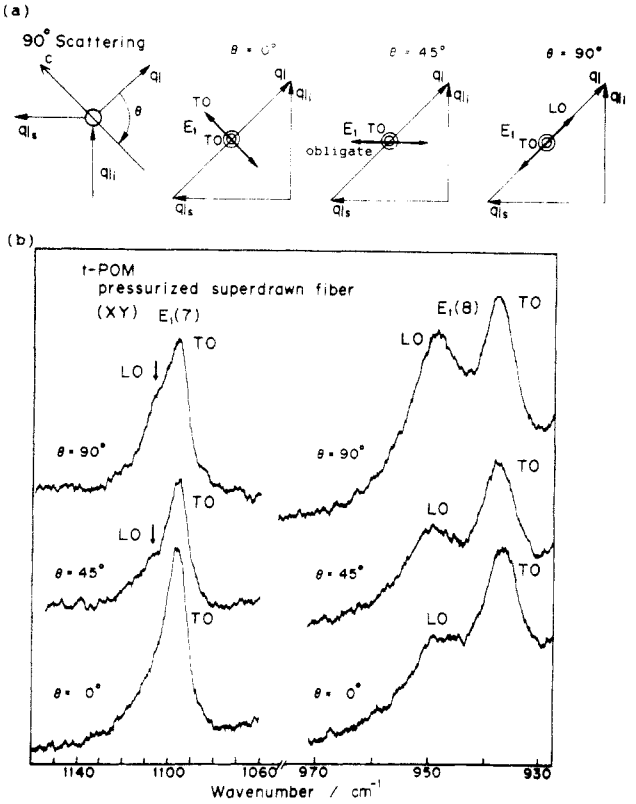

Figure 5. Raman scattering geometries for 90° scattering and angular dispersion of $E_1(7)$ and $E_1(8)$ Raman bands of trigonal poly(oxymethylene). The incident and scattered photon propagation vectors are donoted by $\mathbf{q}_i$ and $\mathbf{q}_s$, respectively, and the phonon propagation vector by $\mathbf{q} = \mathbf{q}_i - \mathbf{q}_s$.

Acknowledgment. We thank Dr. M. Iguchi and Dr. M. Shimomura of the National Institute of Materials and Chemical Research for supplying needlelike single crystals of t-POM and t-POM-d_2. We acknowledge Mr. T. Komatsu of Asahi Chemical Co. Ltd. for supplying pressurized superdrawn filaments of t-POM.

References and Notes

(1) Tadokoro, H.; Yasumoto, S.; Murahashi, S.; Nitta, I. *J. Polym. Sci.* **1960**, *44*, 266.
(2) Uchida, T.; Tadokoro, H. *J. Polym. Sci., Polym. Phys. Ed.* **1967**, *5*, 63.
(3) Carazzolo, G. *J. Polym. Sci., Part A: Gen. Pap.* **1963**, *1*, 1573.
(4) Iguchi, M.; Kanetsuna, H.; Kawai, T. *Makromol. Chem.* **1969**, *128*, 63.
(5) Iguchi, M.; Murase, I. *Makromol. Chem.* **1975**, *176*, 2113.
(6) Iguchi, M. *Br. Polym. J.* **1973**, *5*, 195.
(7) Iguchi, M.; Murase, I. *J. Cryst. Growth* **1974**, *24/25*, 596.
(8) Reneker, D. H.; Geil, P. H. *J. Appl. Phys.* **1960**, *31*, 1916.
(9) Barnes, W. J.; Price, F. P. *Polymer* **1964**, *5*, 283.
(10) Bassett, D. C.; Dammont, F. R.; Salovey, R. *Polymer* **1964**, *5*, 579.
(11) Carter, D. R.; Baer, E. J. *J. Appl. Phys.* **1966**, *37*, 4060.
(12) Tadokoro, H.; Kobayashi, M.; Kawaguchi, Y.; Kobayashi, A.; Murahashi, S. *J. Chem. Phys.* **1963**, *38*, 703.
(13) Nakagawa, K. *J. Polym. Sci., Polym. Lett. Ed.* **1983**, *21*, 933.
(14) Zerbi, G.; Hendra, P. J. *J. Mol. Spectrosc.* **1968**, *27*, 17.
(15) Sugeta, H.; Miyazawa, T.; Kajiwara, T. *Polym. Lett.* **1969**, *7*, 251.
(16) Sugeta, H. Doctral Thesis, Osaka University, 1968.
(17) Kobayashi, M.; Itoh, Y.; Takokoro, H.; Shimomura, M.; Iguchi, M. *Polym. Commun.* **1983**, *24*, 38.
(18) Kobayashi, M.; Morishita, H.; Ishioka, T.; Iguchi, M.; Shimomura, M.; Ikeda, T. *J. Mol. Struct.* **1986**, *146*, 155.
(19) Kobayashi, M.; Morishita, H.; Shimomura, M.; Iguchi, M. *Macromolecules* **1987**, *20*, 2453.
(20) Komatsu, T.; Enoki, S.; Aoshima, A. *Polymer* **1991**, *32*, 1983.
(21) Enoki, S.; Komatsu, T.; Aoshima, A. *Polymer* **1991**, *32*, 1994.
(22) Morishita, H.; Kobayashi, M.; Komatsu, T. *Rep. Prog. Polym. Phys. Jpn.* **1987**, *30*, 131.
(23) Iguchi, M. *Polymer* **1983**, *24*, 915.
(24) Shimomura, M.; Iguchi, M.; Kobayashi, M. *Polymer* **1988**, *29*, 351.
(25) Iguchi, M.; Murase, I.; Watanabe, K. *Br. Polym. J.* **1974**, *6*, 61.
(26) Iguchi, M. *Makromol. Chem.* **1976**, *177*, 549.
(27) Mashimoto, T.; Sakai, T.; Iguchi, M. *J. Phys. D* **1979**, *12*, 1567.
(28) Morishita, H.; Kobayashi, M.; Shimomura, M.; Iguchi, M.; Kuwarahara, H. *Sci. Bull. Fac. Educ., Nagasaki Univ.* **1989**, No. 41, 1.